Biophysical Chemistry 179 (2013) 35–46

Contents lists available at SciVerse ScienceDirect

Biophysical Chemistry

journal homepage: http://www.elsevier.com/locate/biophyschem

IR spectroscopic analyses of amyloid fibril formation of β_2-microglobulin using a simplified procedure for its *in vitro* generation at neutral pH

Heinz Fabian [a,*], Klaus Gast [b], Michael Laue [c], Katharina J. Jetzschmann [b,1], Dieter Naumann [a], Andreas Ziegler [d], Barbara Uchanska-Ziegler [d]

[a] Robert Koch-Institut, ZBS 6, Nordufer 20, D-13353 Berlin, Germany
[b] Institut für Physikalische Biochemie, Universität Potsdam, Karl-Liebknecht-Strasse 24-25, Golm, D-14476 Potsdam, Germany
[c] Robert Koch-Institut, ZBS 4, Nordufer 20, D-13353 Berlin, Germany
[d] Institut für Immungenetik, Charité-Universitätsmedizin Berlin, Freie-Universität Berlin, Thielallee 73, D-14195 Berlin, Germany

HIGHLIGHTS

- Simplified procedure for amyloid fibril formation of β2-microglobulin at neutral pH.
- Analyses of conformational conversions of β2m using IR spectroscopy and EM.
- Early amorphous associates of β2m posses a native-like secondary structure.
- Profound reorganization of secondary and tertiary structures to generate the fibrils.
- Non-native like parallel arrangement of the β-strands in the amyloid fibrils of β2m

GRAPHICAL ABSTRACT

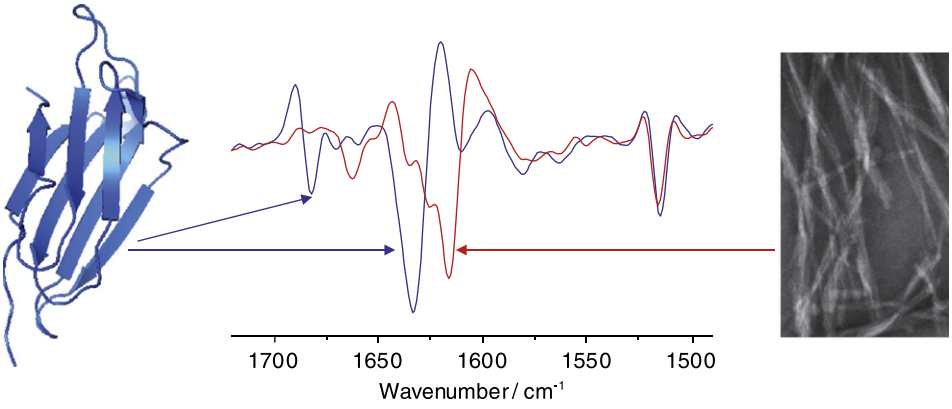

ARTICLE INFO

Article history:
Received 22 March 2013
Received in revised form 29 April 2013
Accepted 1 May 2013
Available online 7 May 2013

Keywords:
Amyloid fibril
β_2-microglobulin
Amyloidogenesis
IR spectroscopy

ABSTRACT

β_2-microglobulin (β_2m) is known to be the major component of fibrillar deposits in the joints of patients suffering from dialysis-related amyloidosis. We have developed a simplified procedure to convert monomeric recombinant β_2m into amyloid fibrils at physiological pH by a combination of stirring and heating, enabling us to follow conformational changes associated with the assembly by infrared spectroscopy and electron microscopy. Our studies reveal that fibrillogenesis begins with the formation of relatively large aggregates, with secondary structure not significantly altered by the stirring-induced association. In contrast, the conversion of the amorphous aggregates into amyloid fibrils is associated with a profound re-organization at the level of the secondary and tertiary structures, leading to non-native like parallel arrangements of the β-strands in the fully formed amyloid structure of β_2m. This study highlights the power of an approach to investigate the formation of β_2m fibrils by a combination of biophysical techniques including IR spectroscopy.

Abbreviations: β_2m, β_2-microglobulin; IR, infrared; SLS, static light scattering; DLS, dynamic light scattering; EM, electron microscopy; DSC, differential scanning calorimetry; ThT, thioflavin T; LS, long straight; WL, worm-like; β_2m-F^{Phys}, β_2-microglobulin fibrils formed at physiological pH; β_2m-F^{Acid}, β_2-microglobulin fibrils formed at acidic pH.

* Corresponding author. Tel.: +49 30 187542202; fax: +49 30 187542606.
E-mail address: fabianh@rki.de (H. Fabian).
[1] Present address: Fraunhofer Institut für Biomedizinische Technik, Am Mühlberg 13, D-14476 Golm, Germany.

0301-4622/$ – see front matter © 2013 Elsevier B.V. All rights reserved.
http://dx.doi.org/10.1016/j.bpc.2013.05.001

1. Introduction

β_2-microglobulin (β_2m) is a 99-residue protein that serves as the non-covalently bound light chain of major histocompatibility complex class I molecules [1]. Native β_2m exhibits a seven-stranded β-sandwich structure organized into two β-sheets connected by a single disulfide bond linking Cys25 and Cys80 [2]. β_2m is also the major component of the amyloid deposits that are found in the musculoskeletal system in patients suffering from dialysis-related amyloidosis (DRA) [3,4]. Although one of the most extensively studied amyloidogenic proteins, the mechanisms by which soluble β_2m is converted into β_2m-amyloid fibrils *in vivo* are not well understood [5,6].

In vitro, wild-type β_2m does not form amyloid-like structures spontaneously at neutral pH [7,8], even at protein concentrations much higher than those commonly found in dialysis patients. Several factors implicated *in vivo*, including the presence of copper ions [9–11], collagen [12], glycosaminoglycans [13,14], lysophosphatic acid [15], non-esterified fatty acids [16,17] and various other substances [18] have been shown to promote and/or induce amyloid fibril formation of β_2m *in vitro* under conditions of physiological pH. Additional factors, such as sodium dodecyl sulphate [19], ultrasonication [20], or the addition of preformed seeds of full-length β_2m [18,21], have been reported to be potent factors that increase the propensity of full-length β_2m to assemble into fibrils under *in vitro* conditions.

Goto and colleagues [22,23] circumvented previously employed procedures by a two-step combination of agitation and heating to generate amyloid fibrils of β_2m. Although lacking the addition of auxiliary substances in comparison to other procedures, this method is still relatively cumbersome.

In this work, we present a simplified stirring/heating approach involving moderately elevated temperatures to convert monomeric β_2m into amyloid fibrils at neutral pH, and we employ it to correlate changes in secondary/tertiary structure with variations in the state of association during different stages of the assembly of β_2m using infrared (IR) spectroscopy, static (SLS) and dynamic light scattering (DLS), and electron microscopy (EM). Our studies provide evidence for a major re-organization during the conversion of β_2m from the native to the fibrillar state.

2. Materials and methods

2.1. Protein expression and purification

β_2m was over-expressed in *Escherichia coli* as inclusion bodies and purified to homogeneity as described previously [24]. An N-terminal initiating Met residue (Met0) was incorporated into 95% of β_2m prepared by this method. The purified protein was extensively dialyzed against water and lyophilized. For the experiments, the lyophilized protein was dissolved in buffer (10 mM sodium cacodylate, pH 7.5) containing varying concentrations of NaCl. The concentration of the protein samples was determined spectrophotometrically at 280 nm ($A^{1\ cm}_{1\%} = 16.17$) [25].

2.2. Infrared spectroscopy

The protein solutions were placed into demountable CaF_2 IR-cells [26] with an optical pathlength of 50 μm for measurements in D_2O buffer. Infrared spectra were recorded with Bruker IFS-28B and Bruker IFS-66 Fourier transform infrared (FTIR) spectrometers equipped with deuterated triglycine sulphate (DTGS) detectors and continuously purged with dry air. For each sample, 128 interferograms were co-added and Fourier-transformed to yield spectra with a nominal resolution of 4 cm^{-1}. The sample temperature was controlled by means of a thermostated cell jacket [26]. In order to minimize problems due to base line drifts of the spectrometer or variations of the dry atmosphere in the spectrometer, the sample in the cell jacket was mounted in a motor-driven sample shuttle, which allowed the recording of the background immediately before recording of the sample spectrum without opening the sample chamber of the spectrometer. Solvent spectra were recorded under identical conditions and subtracted from the spectra of the proteins in the relevant solvent and at the relevant temperature. Spectral contributions from residual water vapor, if present, were eliminated using a set of water vapor spectra. In this way, IR spectra with a very high signal-to noise ratio were obtained, even at relatively low protein concentrations of only 0.5–1 mg/mL. The final unsmoothed protein spectra were used for further analysis. Band positions and band intensities were determined by standard functions of the Bruker OPUS software, that were implemented into home-built macros for data analysis. Second derivatives were obtained using the Savitzky–Golay algorithm with 13-point smoothing. Band-narrowing by Fourier self-deconvolution was performed under OPUS applying a Lorentzian line shape function with a bandwidth of 2.6 and a band-narrowing factor of 2. Intensity and frequency profiles, respectively, of the IR data as a function of temperature and/or time were created using the ORIGIN software from second derivative spectra. Extracting intensity changes from second derivative spectra has limitations, because sharp bands are enhanced at the expense of broad ones, thus not preserving the integrated intensities of the bands. However, as long as the bands of interest are well separated and the band widths of the corresponding bands change at best only marginally and similarly during the investigation of protein conformational changes, this approach was found to be applicable for comparative evaluations of transition profiles [27].

2.3. Laser light scattering

SLS and DLS data were measured simultaneously with one and the same instrument at a scattering angle of 90° [28]. For measurements of salt-induced changes, appropriate amounts of pre-filtered stock solutions were mixed with salt-free protein within the quartz cells (Hellma 105.251-QS), equipped with a magnetic stirrer. The sample temperature was regulated by a Peltier controller.

2.4. Light scattering and ThT fluorescence measurements

Light scattering was also monitored with a Varian Cary Eclipse spectrofluorometer using a quartz cell (Hellma 105.251-QS), with a light path of 3 mm. For light scattering, the wavelengths for excitation and emission were both set at 500 nm. The temperature of the sample solutions was kept at the corresponding temperatures by a Peltier controlled cell holder, equipped with a magnetic stirrer. Thioflavin T (ThT) fluorescence was monitored with a Fluorolog Horiba Jobin Yvon spectrofluorometer using a quartz cell with a light path of 5 mm. The fluorescence was exited at 440 nm and the emission was recorded between 450 and 600 nm.

2.5. Transmission electron microscopy

Sample preparation and analysis were done as previously described [29]. Briefly, suspensions were adsorbed at bacitracin-treated surfaces of standard sample supports (formvar and carbon coated copper grid) and negatively stained with uranyl acetate. Samples were analyzed by using a transmission electron microscope at 120 kV (Tecnai Spirit, FEI Co., USA) that was equipped with a 1 k CCD camera.

3. Results

3.1. Thermal denaturation of β_2m at neutral pH probed by IR spectroscopy

In order to analyze the secondary structure and thermal stability of β_2m, we first recorded IR spectra of the protein in D_2O buffer at pH 7.5 at protein concentrations of ~7 mg/mL (Fig. 1A) and ~1 mg/mL

(Fig. 1B), as well as at ~1 mg/mL in the presence of 1 M NaCl (Fig. 1C). All studies were carried out with fully hydrogen/deuterium (H/D)-exchanged samples, assuring that the spectral changes observed as a function of temperature solely reflect structural changes due to thermal denaturation of the proteins. Exchange of all amide protons with deuterons was achieved by keeping the protein solutions overnight at 37 °C. It was verified by the absence of the amide A band at ~3300 cm^{-1} in the protein IR spectra [29]. To better visualize weak spectral features, the second derivatives of the IR spectra were calculated, where the minima correspond to absorption maxima or shoulders in the measured spectra.

The low-temperature IR spectra of β_2m at the three experimental conditions given in Fig. 1 were indistinguishable, and dominated by a major amide I band component at 1633 cm^{-1} and a weaker band component at 1682 cm^{-1}, both together indicating the presence of intramolecular antiparallel β-sheet structures, in agreement with previous IR studies [29–31]. Weak features at 1670 and 1660 cm^{-1} in the spectra of the natively folded protein can be assigned to turn-like structures, while the IR bands between 1480 and 1600 cm^{-1} are due to amino acid side chain absorptions [29,30]. Among the latter, the well separated tyrosine band at ~1515 cm^{-1} is a useful internal standard to normalize the IR spectra of a protein measured under different conditions [30,32]. The spectra measured between 25 °C and 60 °C were also very similar to each other, indicating only minor changes in secondary structure over this temperature range.

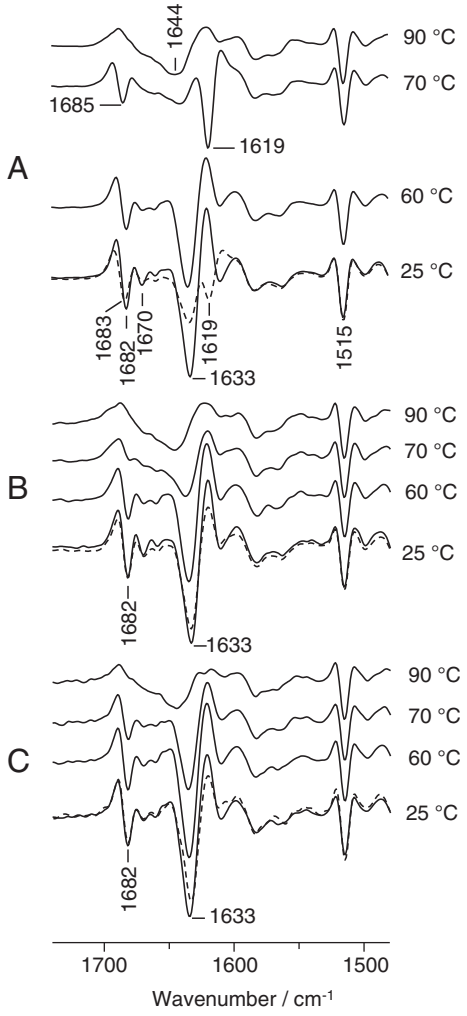

Fig. 1. Analysis of β_2m by infrared spectroscopy. IR spectra (second derivatives) of β_2m in deuterated sodium cacodylate buffer (10 mM, pH 7.5) were obtained at protein concentrations of (A) ~7 mg/mL, (B) ~1 mg/mL, and (C) ~1 mg/mL in the presence of 1 M NaCl at the indicated temperatures. The dashed lines correspond to the spectra obtained after heating the corresponding sample from 25 to 90 °C and then cooling back to 25 °C.

In contrast, the spectra measured at 60 °C and 70 °C were quite different, demonstrating that major structural changes occurred over this temperature range. In the 70 °C spectrum of β_2m at a protein concentration of ~7 mg/mL (Fig. 1A), the β-sheet band component at 1633 cm^{-1} was absent, and the spectrum was now dominated by a major amide I band component at 1619 cm^{-1} and a weaker band component at 1685 cm^{-1}, indicating that at this relatively high protein concentration the native intramolecular β-sheet structure of β_2m had been converted into an intermolecular assembly (see also Fig. 2A). The characteristic β-aggregate band at 1619 cm^{-1} almost disappeared upon further temperature increase to 90 °C, while the nearly featureless amide I band contour centered at 1644 cm^{-1} (Fig. 1A), suggesting a predominantly unfolded protein structure at 90 °C. However, the β-aggregate band at 1619 cm^{-1} was again visible in the spectrum obtained after cooling the protein sample from 90 °C down to 25 °C (dashed line in Fig. 1A), indicating that the thermal denaturation of β_2m at a protein concentration of ~7 mg/m was partly irreversible. EM micrographs of this sample revealed an amorphous morphology without ordered structures (data not shown).

A decrease in protein concentration to ~1 mg/mL, however, led to a clear change in the denaturation behavior of β_2m (Fig. 1B). No β-aggregate bands were observed at any temperature between 60 and 90 °C (for brevity, only the spectrum obtained at 70 °C is shown in Fig. 1B). Furthermore, the spectra obtained at 25 °C before heating and after cooling from 90 °C down to 25 °C (the solid and dashed lines, respectively, at 25 °C in Fig. 1B) were similar, suggesting that no significant irreversible β-aggregation occurred upon thermal unfolding of β_2m at a protein concentration of ~1 mg/mL. At this protein concentration, the addition of NaCl appeared to stabilize the structure of β_2m, and no indications for aggregation were observed upon denaturation (Fig. 1C). The transition temperatures calculated from the intensity/temperature plot of the β-sheet band at 1633 cm^{-1} revealed an increase from 66 °C to 71 °C upon the addition of 1 M NaCl (Fig. S1). Such an increase in the melting point of β_2m is in agreement with DSC studies reported recently [25].

3.2. Stirring-induced association of β_2m at 37 °C and preliminary conversion tests

We then tried to convert monomeric β_2m into amyloid fibrils at physiological pH by combining stirring and heating, mainly following the two-step conversion procedure described by Goto and colleagues [22,23]. Under our experimental conditions, β_2m was agitated first at 37 °C for 24 h in the quartz cell of a spectrofluorometer equipped with a magnetic stirrer. Aliquots were then taken out for subsequent heating-cooling cycles from 20 to 90 °C in the IR cell without stirring, and IR spectra at selected time-points were recorded. The experiments were carried out at protein concentrations of 0.5–1 mg/mL, conditions under which no indications for irreversible aggregation upon thermal denaturation had been observed before (Fig. 1C). The IR spectrum of the sample obtained after 24 h of stirring in the quartz cell (solid line, Fig. 2A) was very similar to the spectrum obtained without stirring (dashed line, Fig. 2A), indicating a primarily native-like secondary structure after this treatment. At the same time, EM micrographs of the sample revealed some stirring-induced association of β_2m molecules into amorphous aggregates (Fig. 2B).

An aliquot (15 μL) of the aggregated β_2m sample formed by mildly stirring the protein solutions at 37 °C in the presence of 1 M NaCl in the quartz cell was then taken out for analysis by IR spectroscopy. The IR spectrum obtained after the first heating-cooling cycle (solid line, Fig. 2C) was still dominated by the native-like β-sheet structure features at 1633 and 1682 cm^{-1}. After several heating-cooling cycles between 25 °C and 90 °C, a loss of spectral intensity at 1633 cm^{-1}, accompanied by an intensity increase at 1619 cm^{-1}, was observed

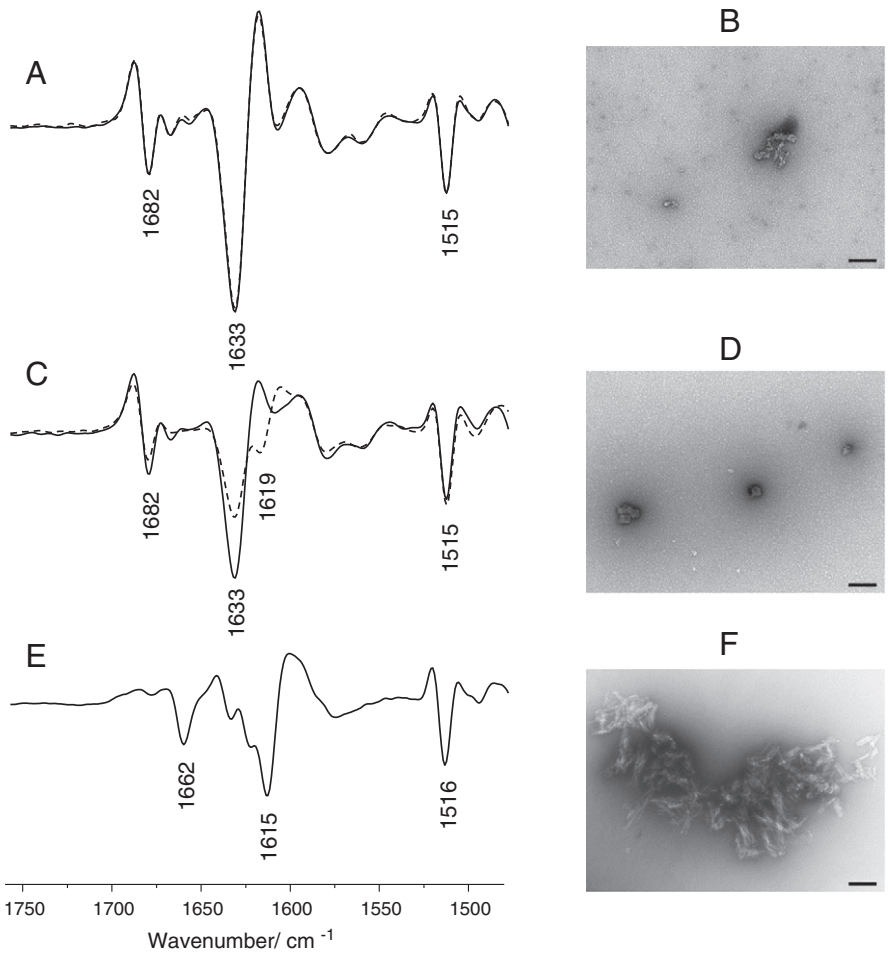

Fig. 2. Stirring-induced association of β_2m in D_2O buffer in the presence of 1 M NaCl. (A) IR spectra (second derivatives) of an aliquot before (dashed line) and after 24 h of stirring (solid line) at 37 °C in the quartz cell. (B) EM micrograph of amorphous aggregates produced by 24 h stirring at 37 °C. (C) IR spectra of an aliquot obtained after 24 h of stirring in the quartz cell for IR analysis and subsequent first heating in the IR cell (solid line) and after five heating-cooling cycles between 25 and 90 °C in the IR cell (dashed line). (D) EM micrograph of the sample after five heating-cooling cycles between 25 and 90 °C in the IR cell. (E) IR spectrum of an aliquot taken out after two-step stirring in the quartz cell (24 h at 37 °C, followed by 2 h at 70 °C). (F) EM micrograph of amyloid fibrils of β_2m produced by the two-step stirring procedure in the quartz cell. The black bars in the micrographs represent 200 nm.

(dashed line, Fig. 2C), indicating a partial transformation of native-like secondary structure into intermolecular aggregates. However, EM micrographs of the heat-induced species revealed no evidence for fibril structures, but only compact associates (Fig. 2D).

In our search for conditions to obtain amyloid fibrils of β_2m, we continued with stirring the protein sample that remained in the quartz cell, but now at a temperature of 70 °C. This treatment led to drastic conformational changes of the protein molecules. Their IR spectrum was dominated by a major amide I band component at 1615 cm^{-1} and a weaker feature at 1662 cm^{-1} (Fig. 2E). It was, thus, clearly different from the spectrum of the native protein (Fig. 1A) or those of the heat-induced amorphous species (dashed line in Fig. 1A and Fig. 2C). EM micrographs of the assemblies with the characteristic IR spectrum shown in Fig. 2E now revealed the presence of amyloid fibrils (Fig. 2F).

3.3. Systematic conversion experiments of monomeric β_2m into amyloid fibrils

This promising result prompted us to study the impact of different experimental factors on the fibril formation of β_2m at elevated temperatures more systematically and to establish a procedure that would allow us to analyze the conversion events by our combined experimental approach. For legibility, an overview of the different experimental conditions applied in this work to convert β_2m molecules into different forms of associates, together with major results, is given in Table 1.

The analysis of the diffusion coefficients of the protein by dynamic light scattering (DLS) revealed no significant concentration dependence at 25 °C (Fig. S2), and the extrapolation to zero protein concentration leads to Stokes radii of 1.94 nm and 2.05 nm in the absence and presence of 1 M NaCl, respectively, indicating the initial presence of monomeric β_2m under both conditions. Control experiments at 65 °C with β_2m solutions (protein concentration 0.7 mg/mL) containing 1 M NaCl, but in the absence of stirring, showed only a minor conversion into intermolecular associates, and provided no evidence for fibril formation after 24 h (data not shown). The stirring-induced association behavior of the protein at neutral pH and intermediate temperatures of 60–70 °C was complicated by a strong tendency of the molecules to form occasional large aggregates, and a notable precipitation of these aggregates in the quartz cell. This prevented us from performing a detailed analysis of the hydrodynamic parameter changes by DLS, such as described before for the association of β_2m at acidic conditions [29].

As a consequence, we only analyzed the increase in light scattering intensity associated with aggregation by agitation at different stirring rates. In order to optimize the conditions for fibril formation at elevated temperatures and in the presence of 1 M NaCl, stirring rates of 1000, 700, and 350 rpm, were applied. Stirring experiments at 65 °C revealed a clear dependence of the aggregation behavior of

Table 1
Conversion of β_2m at physiological pH.

Experimental conditions	Secondary structure (IR)	Association (DLS)	EM morphology/ThT binding
25 °C or 1 M NaCl, 25 °C	Native structure (see Fig. 1B & C)	Monomer (see Fig. S2)	n.d./ no binding
90 °C or 1 M NaCl, 90 °C	Unfolded structure (see Fig. 1B &C)	n.d.	n.d.
1 M NaCl, 37 °C, 24 h stirring	Native-like structure (see Fig. 2A)	n.d.	Compact associates/no binding (see Fig. 2B)
1 M NaCl, 37 °C, 24 h stirring, followed by 5 heating-cooling cycles between 25 and 90 °C in the IR cell	Mixture of native-like and antiparallel intermolecular β-sheet structures (see Fig. 2C)	n.m.	Compact associates/binding n.m. (see Fig. 2D)
1 M NaCl, 65–70 °C, 3.5 h stirring	Mixture of native-like and parallel β-sheet structures	Conglomerates of 20–50 nm diameter	Primarily amorphous associates, few fibrils/weak binding
1 M NaCl, 65 °C, 3.5 h stirring, followed by heating to 90 °C in the IR cell	Parallel β-sheet structure (see Fig. 2E)	n.m.	Amyloid fibrils/strong-binding (see Fig. 2F)
[a]**1 M NaCl, 60–70 °C, 24 h stirring**	**Parallel β-sheet structure** (see Fig. 4A)	**n.m.**	**Amyloid fibrils/strong binding** (see Fig. 5)
1 M NaCl, 65 °C, 20 h, no stirring	Native-like structure	minor tendency for association	Very weak binding

Protein concentrations: 0.5–1 mg/mL; n.d., not determined; n.m., not measurable.
[a] Bold script, simplest procedure leading to amyloid fibril formation.

the protein on the stirring rate (Fig. 3). At 1000 rpm (Fig. 3A), only loosely packed aggregates were formed over 3.5 h (Fig. 3B), which could not be converted into fibrillar structures by subsequent heating of the sample for 2 h at 70 °C without stirring (data not shown). At a stirring rate of 700 rpm, amorphous aggregates as well as short bundles of fibrils were found after 3.5 h (Fig. 3C). Subsequent heating of this sample for 2 h at 70 °C clearly leads to further conformational changes that were associated with ThT-binding (data not shown), and EM micrographs now dominated by fibrils (Fig. 3D). As the stirring rate was further decreased to 350 rpm, primarily amorphous associates together with some fibril-like species (Fig. 3E) were also found after 3.5 h. An aliquot of the β_2m sample taken out of the quartz cell after stirring for 3.5 h at 65 °C could be fully converted into amyloid fibrils by subsequent heating to 90 °C within the IR cell (Fig. 3F). Finally, β_2m molecules were fully converted into amyloid fibrils by continuous stirring with 350 rpm for 18 h at 65 °C, as demonstrated by a drastic enhancement of the ThT fluorescence following a lag phase of 3–4 h (Fig. 3G) and by an EM micrograph obtained afterwards (Fig. 3H).

Stirring-induced fibril formation of β_2m was found to be also feasible at 60 °C, but the lag phase was increased by 2–3 h when compared with the studies carried out before at higher temperatures (see, *e.g.*, Fig. 3G). This slow-down of the event provided good conditions to monitor the conversion process by a combined IR/EM approach. For our purpose, the β_2m sample was stirred at 60 °C in the quartz cell of the spectrofluorometer for 24 h, the event was monitored by increasing light scattering, and aliquots of 50 μL were taken out of the cell at certain time points for parallel and immediate (within minutes) characterization by IR spectroscopy (Fig. 4) and preparation of the samples for EM (Fig. 5).

Although the amplitudes of the observed spectral changes were only in the milliabsorbance range (Fig. 4A), the excellent signal-to noise ratio of our IR spectra permitted us to analyze the conversion of β_2m from the native to the fibrillar state based on absorbance and frequency changes of selected IR marker-bands (Fig. 4B and 4C). Practically no changes in secondary structure were observed within the first 4 h of stirring at 60 °C (Fig. 4B), although numerous amorphous aggregates in the sample were already detected at that time by EM (Fig. 5A). Major structural changes in secondary and tertiary structures occurred between 6 and 8 h, however, as demonstrated by a complete loss of the native-like β-sheet band component at 1633 cm^{-1} after 8 h, a concomitant strong increase of the intermolecular β-sheet amide I band component at 1615 cm^{-1}, and a shift in peak position of the tyrosine band at ~1515 cm^{-1} (1515.0 cm^{-1} in the initial state to1516.2 cm^{-1} after 10 h). The observed shift of the tyrosine side chain band indicates that most likely all of the six tyrosine residues present in β_2m experience major changes in their respective microenvironment (changes in tertiary structure) between 6 and 10 h. These changes and the formation of the intermolecular β-sheet structure exhibited almost identical kinetics (compare the red dots and black stars in Fig. 4B).

Both events came to completion after ~10 h, thus taking 2 h more than the disruption of the native-like secondary structure of β_2m (blue dots in Fig. 4B). EM micrographs of the assemblies obtained after 8 h revealed the presence of long and straight amyloid fibrils (Fig. 5C), and numerous clumps of fibrils were observed after stirring for up to 24 h (Fig. 5D). Those fibril structures were not amenable to further heat-induced structural changes, as indicated by identical IR spectra obtained before and after heating to 90 °C (compare the red and black traces in Fig. 4D), and only minor spectral differences upon heating to 90 °C (Fig. 4D, green trace).

These systematic studies, that are summarized in Table 1 illustrate that stirring of β_2m at elevated temperatures between 60 °C and 70 °C and in the presence of 1 M NaCl is an efficient and relatively simple way to obtain amyloid fibrils of this protein at physiological pH values (conditions highlighted in bold letters in Table 1). A similarly efficient conversion of β_2m into fibrils by stirring at 65 °C was also achieved at a reduced salt concentration of 0.5 M NaCl (Fig. S3A). Moreover, the conversion approach described here for the first time does not seem to be restricted to experiments in sodium cacodylate buffer, but is also applicable for the more commonly used phosphate buffer, as shown by a stirring experiment performed in phosphate buffer at 70 °C and in the presence of 1 M NaCl (Fig. S3B).

3.4. Comparison of morphological and structural features of amyloid fibrils of β_2m obtained at neutral and acidic pH

Transmission electron micrographs showed the presence of long straight (LS) fibrils for the assemblies prepared at neutral pH (β_2m-F^{Phys}) (Fig. 6A) as well as for those formed at acidic pH of 2.1 (β_2m-F^{Acid}) (Fig. 6B), although some morphological differences could be observed. Typical for the β_2m-F^{Acid} species was a pronounced twisted fine structure with relatively regular periodicity of ~100 nm, in agreement with the results described by other authors for mature β_2m fibrils formed at low pH [33]. In contrast to that, the β_2m-F^{Phys} species appeared thicker and less twisted. Moreover, this species showed a tendency to associate laterally, as observed for the fibrils of β_2m prepared at neutral pH by the two-step conversion

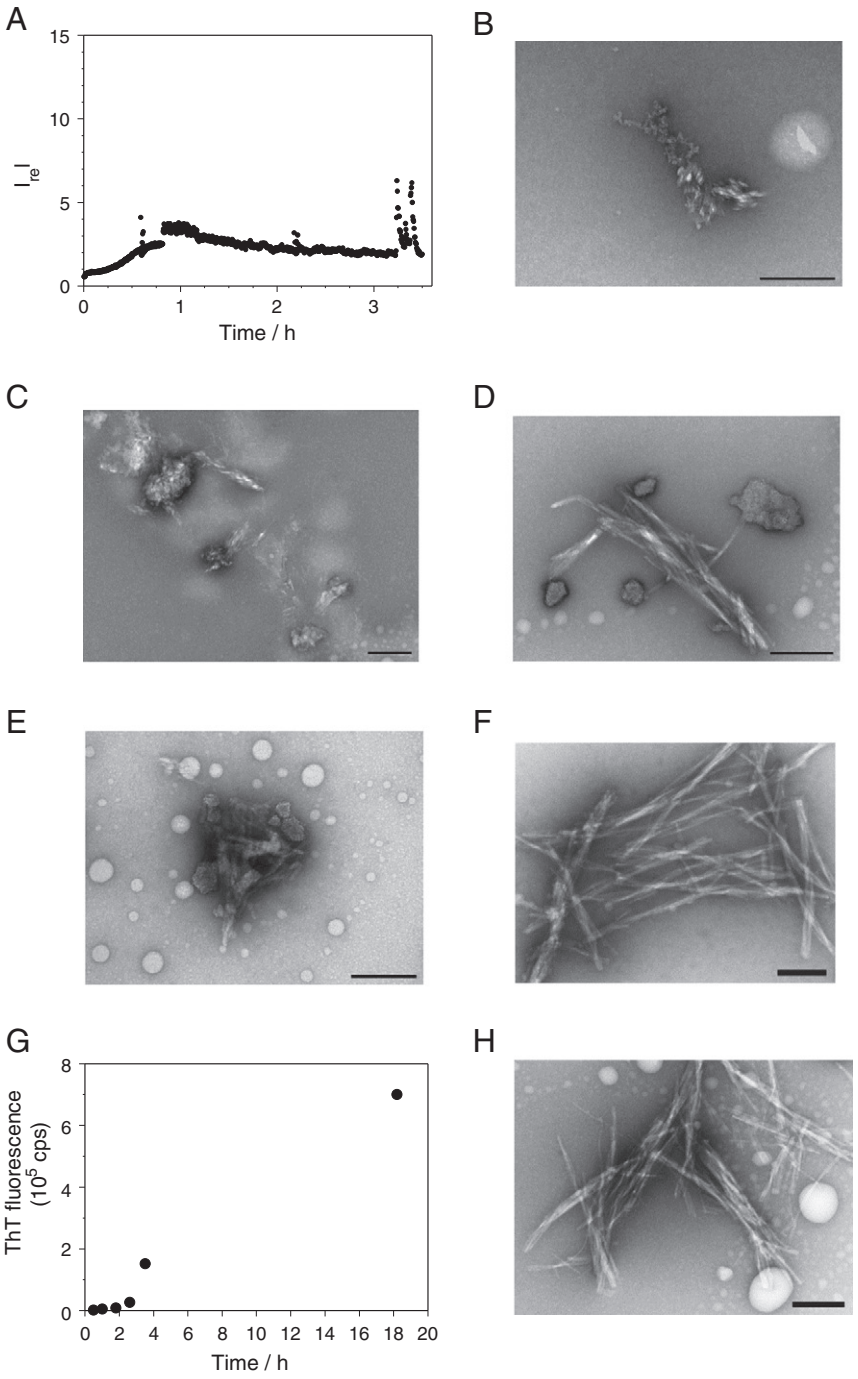

Fig. 3. Stirring rate dependence of the association of β_2m in D_2O buffer in the presence of 1 M NaCl at 65 °C. (A) Increase in light scattering at 500 nm at a stirring rate of 1000 rpm. (B) EM micrograph of structures formed after stirring with 1000 rpm for 3.5 h. (C) EM micrograph of structures formed after stirring with 750 rpm for 3.5 h. (D) EM micrograph of fibrillar structures formed after stirring with 750 rpm for 3.5 h and subsequent heating for 2 h at 70 °C without stirring. (E) EM micrograph of structures obtained after stirring with 350 rpm for 3.5 h. (F) EM micrograph of fibrils obtained by a two-step procedure (3.5 h stirring with 350 rpm at 65 °C), followed by heating to 90 °C in the IR cell and cooling to 25 °C. (G) ThT fluorescence intensity in sample aliquots taken out of the quartz cell at selected time points during stirring of the sample for 18 h with 350 rpm at 65 °C. (H) EM micrograph of fibrils formed in the β_2m sample after stirring for 18 h with 350 rpm at 65 °C. The black bars in the micrographs represent 200 nm.

procedure described by Sasahara et al. [22]. Subtle pH-specific morpho logical differences, such as presented here for β_2m-F^{Phys} and β_2m-F^{Acid}, were also described recently for fibrils of lysozyme formed at pH 7.5 and pH 2.0 [34].

For a comparison of structural features, IR spectra of various forms of β_2m are shown in Fig. 7, all measured as fully deuterated samples. The IR spectral characteristics of β_2m-F^{Phys} turned out to be very similar to those of β_2m-F^{Acid} which we had described previously [29], indicating closely related secondary structures of the two species. Strikingly, both β_2m-F^{Phys} (Fig. 7A) and β_2m-F^{Acid} (Fig. 7B) exhibited no IR band component at ~1682 cm^{-1} in their spectra. In the case of β_2m-F^{Acid}, we previously took the absence of the spectral component at ~1682 cm^{-1} as an indication for a parallel arrangement of the β-strands in this sample [29].

In line with this assumption, no prominent feature attributable to a high-frequency β-band component was observed in the IR spectra of natively folded barstar (Fig. S4A). Barstar is a protein composed of four helices and a three-stranded parallel β-sheet [35]. Likewise, a well-resolved high frequency band component is absent from the IR spectrum of triose phosphate isomerase [36], consistent with its

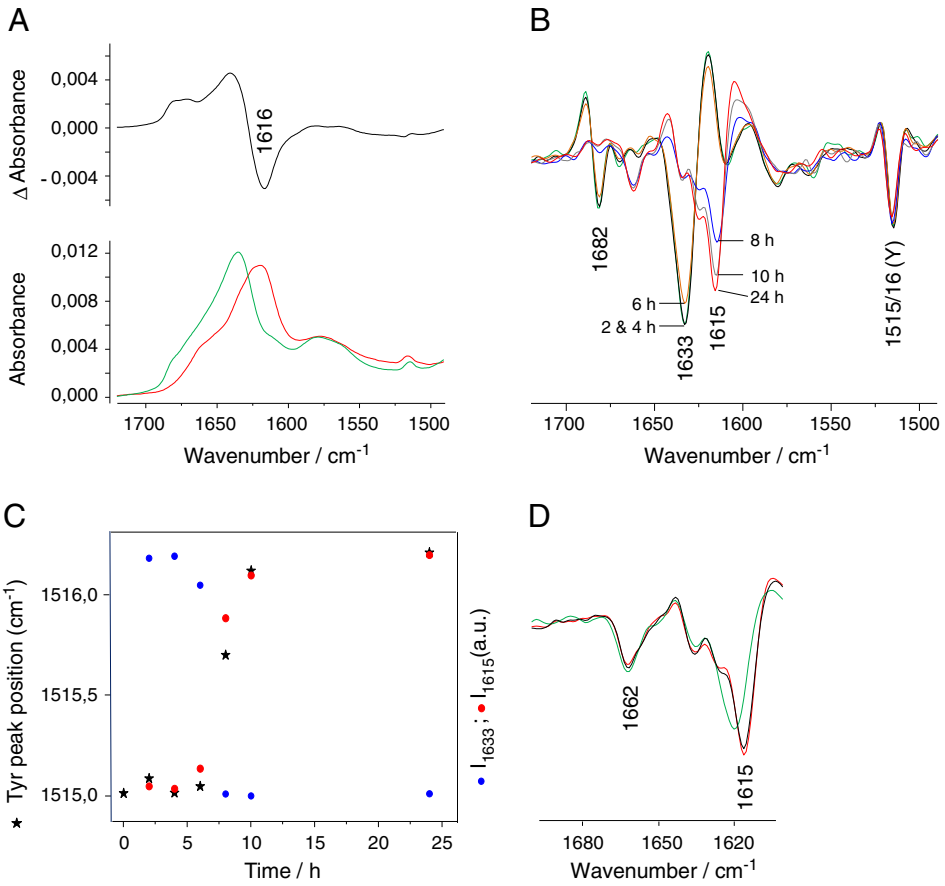

Fig. 4. Structural characterization of the stirring-induced conversion of β_2m into amyloid fibrils at 60 °C in the presence of 1 M NaCl in the quartz cell of a spectrofluorimeter. (A) IR absorbance spectra of natively folded β_2m before stirring (green trace) and of β_2m amyloid fibrils obtained after stirring for 24 h at 60 °C (red trace). The upper black trace shows the corresponding IR difference spectrum (before stirring minus after stirring) (B) IR spectra (second derivatives) of aliquots of the sample taken out at six time points (2 h, green trace; 4 h, black trace, 6 h, brown trace, 8 h, blue trace, 10 h, gray trace, 24 h, red trace) after stirring at 60 °C in the quartz cell and measured in the IR cell at room temperature afterwards. (C) Kinetics of the event, monitored by measuring the intensity loss (taken from second derivative spectra) of the native-like β-sheet band component at 1633 cm^{-1} (blue dots), the increase of the intermolecular β-sheet intensity at 1615 cm^{-1} (red dots), and the shift in position of the tyrosine band at ~1515 cm^{-1} (black stars). (D) IR spectra of an aliquot of β_2m fibrils measured at 25 °C (red trace) and 90 °C (green trace). The black trace corresponds to the sample after heating to 90 °C and cooling down to 25 °C in the IR cell.

parallel β-sheet structure. Recently, direct proof for a parallel in-register arrangement of β-strands in long straight fibrils of β_2m formed under acidic conditions came from magic angle spinning NMR [37] and electron paramagnetic resonance experiments [38]. The latter report provided also evidence that the WL particles of β_2m do not adopt a parallel arrangement, such as observed for the LS fibrils. The close relationship of the IR spectroscopic observations described above for β_2m-F^{Acid} and β_2m-F^{Phys} suggests that a parallel organization of β-strands is also characteristic for the fibrils of β_2m prepared at neutral pH in the present work.

In contrast to that, the IR spectrum of worm-like (WL) assemblies of β_2m (Fig. 7C) revealed a well-defined component at 1684 cm^{-1}, but with an additional strong component at 1616 cm^{-1}, indicating that the non-native intermolecular structure of the WL species involves an antiparallel arrangement of the β-strands.

Apart from the very similar overall IR spectral features of β_2m-F^{Phys} (Fig. 7A) and β_2m-F^{Acid} (Fig. 7B), the respective spectra showed also some subtle differences, *e.g.*, a 4 cm^{-1} difference in peak position (1615 *vs* 1619 cm^{-1}) of the low-frequency β-sheet band component. These results point to subtle structural differences between the β-sheets present in β_2m-F^{Acid} and β_2m-F^{Phys}, which might arise from differences in hydrogen-bonding or in the planarity of the β-sheets [39], as well as distinctions in the number of strands per sheet [40,41], in the stacking of β-sheets, or in the stack size [42]. Minor pH-dependent spectral differences were also observed for weaker features between 1625 and 1640 cm^{-1} and between 1650 and 1665 cm^{-1}. The attributes around 1630 cm^{-1} in the spectra of the β_2m fibrils could suggest the presence of some residual native-like β-sheet structure in the amyloid samples, because their positions coincide with the dominant bands observed for β_2m in its native fold (Fig. 7D). However, we regard this as unlikely, because a corresponding high-frequency β-sheet component due to a native-like antiparallel arrangement of the β-strands could not be observed consistently in all fibril spectra. Although we cannot exclude that the weak features between 1625 and 1640 cm^{-1} in the spectra of the β_2m amyloid fibrils point to some heterogeneity of the β-sheet structure(s) in the amyloid fibrils of β_2m, we would like to consider the assignment of the features between 1625 and 1640 cm^{-1} in the spectra of the amyloid fibrils as uncertain at the moment. This is also true for the assignment of the spectral features at ~1662 cm^{-1} in the spectra (Fig. 7A and B). Possibly, the band components between 1625 and 1640 cm^{-1} and between 1650 and 1665 cm^{-1} reflect an arrangement of β-strands in the fibrils, which cannot be specified based on currently known structure–spectrum correlations for natively folded proteins.

4. Discussion

This study is part of our efforts to explore conformational changes associated with the assembly of β_2m. We had originally probed the

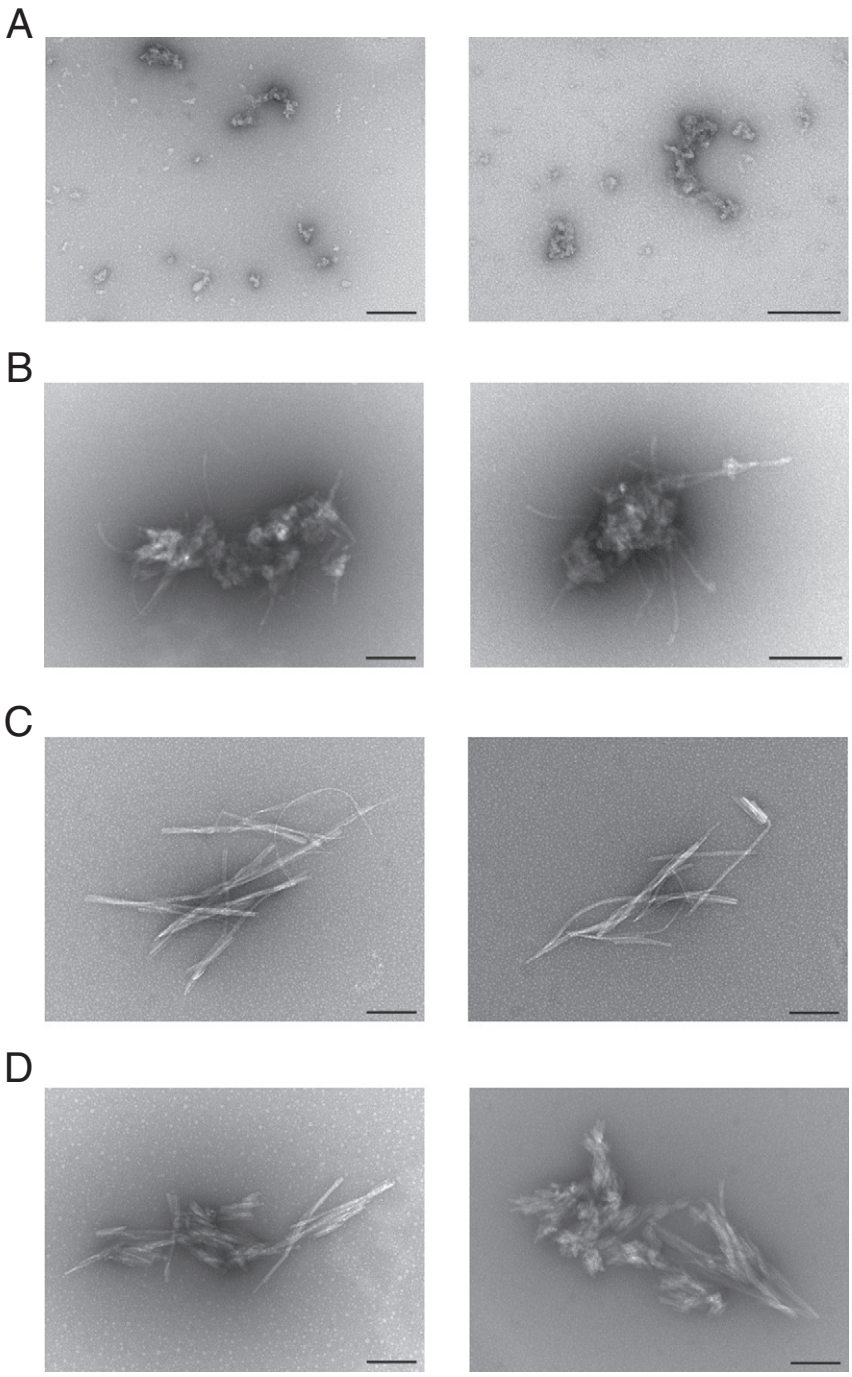

Fig. 5. Morphological characterization of the stirring-induced conversion of β_2m into amyloid fibrils at 60 °C in the presence of 1 M NaCl in the quartz cell. EM micrographs of aliquots taken out (A) 2 h, (B) 6 h, (C) 8 h, and (D) 24 h after induction of the event. Two typical micrographs are shown for each time point. The black bars in the micrographs represent 200 nm.

formation of amyloid fibrils at low pH, and provided evidence for a non-native-like secondary structure as characteristic for amyloid fibrils of β_2m under these conditions [29]. Here we succeed in producing amyloid fibrils of β_2m at physiological pH values *via* an efficient and relatively simple one-step procedure, a modification of the agitation-heating two-step method originally described by Goto and co-workers [22].

Following the strategy of these workers, we tried to convert amorphous aggregates of β_2m obtained by stirring for 24 h at 37 °C into amyloid fibrils by several heating-cooling cycles between 25 °C and 90 °C. These experiments were performed in an IR cell, because this approach would have allowed us directly to monitor changes in secondary and tertiary structures during the conversion process by analyzing the accompanying spectral changes. However, these attempts to convert the amorphous aggregates of β_2m into amyloid fibrils failed (Fig. 2C and D), for unclear reasons. It might be that the specific conditions for a minute protein sample between two CaF_2 windows that are separated by only 50 μm are not comparable to the conditions in the sample chamber of a DSC instrument as used by Sasahara and co-workers [22].

We did, however, find that the stirring of a β_2m solution at temperatures around β_2m's transition temperature is a reliable procedure to convert natively folded β_2m molecules into amyloid fibrils. Moreover,

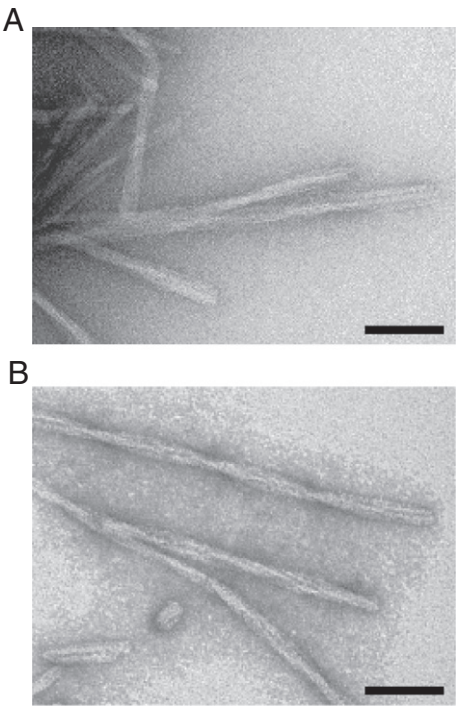

Fig. 6. Comparison of morphological properties of β_2m-fibrils. (A) EM micrograph of fibrils prepared at neutral pH in this work (β_2m-F^{Phys}). (B) EM micrograph of fibrils formed at acidic pH (β_2m-F^{Acid}) (EM data taken from previous work by our group, Ref. [29]). The black bars in the micrographs represent 100 nm.

the experimental conditions applied permit the analysis of β_2m conversion from the native to the fibrillar state using a combination of IR spectroscopy and EM microscopy, an experimental approach, which had already successfully been applied by other authors when experimentally following the formation of bovine insulin amyloid fibrils [43]. IR spectroscopy has the advantage of being invulnerable to artifacts from light scattering, such as in CD spectroscopy, and is, thus, particularly useful in studying structural conversions associated with aggregation processes. In a specially developed apparatus, the joint application of IR and SLS offers the potential for the quasi-simultaneous measurement of changes in secondary structure (IR) and particle growth (SLS) [44].

Under our experimental conditions, mild agitation of the β_2m molecules that are mainly unfolded at the elevated temperature using a magnetic stirrer turned out to be very effective to convert the protein into fibrils (Fig. 3). The conversion begins with the formation of relatively large and less defined aggregates (Fig. 5A), whose secondary structure is primarily native-like (Fig. 4B). After a lag phase, major changes in secondary and tertiary structures occur upon the continuation of the procedure, finally leading to β_2m associates with morphology (Fig. 3H, Fig. 5C and D) and ThT binding features (Fig. 3G), that are characteristic of mature amyloid fibrils. Interestingly, β_2m samples taken out of the quartz cell some hours after treatment, primarily amorphous associates together with some fibril-like species (Fig. 3E), could be fully converted into amyloid fibrils by heating this sample within the IR cell afterwards, but without stirring (Fig. 3F). This indicates that already a relatively short heat-and-stirring-treatment of the sample can generate amyloid templates, that are likely to act as seeds for fibril formation of the so-far native-like β_2m molecules upon their thermal unfolding. Such templates could be potent factors to stimulate β_2m molecules to assemble into fibrils *in vivo* under destabilizing local conditions.

The IR spectra of all β_2m amyloid fibrils obtained in this work show strong low-frequency β-sheet band components at 1615 cm^{-1} (Figs. 2E, 4D, 7A) but lack a high-frequency β-band component at 1680–1690 cm^{-1}. We regard this characteristic in the IR spectra of the LS fibrils as an indicator for a parallel organization of the fibrillar β-strands. It is notable that a high-frequency β-band component is also only very weak or even absent in the IR spectra of LS fibrils of other proteins, such as insulin [43], SH3 domain [45,46], lysozyme [47], α-synuclein [36], amyloid β-peptides [48,49], or peptide models [50,51]. Moreover, similar results are obtained upon IR spectroscopy of natively folded barstar (Fig. S4A) and of triose phosphate isomerase [36], both proteins known to contain β-sheet structural segments characterized solely by a parallel arrangement of their β-strands. In contrast, a high-frequency component is prominent in the spectra of other protein assemblies, such WL particles, oligomers [29,31,45,46,49], and amorphous associates. These IR data indicate that mature amyloid fibrils, on one side, and pre-fibrillar or amorphous species on the other side, adopt different secondary structures. In the case of β_2m, direct proof for a parallel in-register arrangement of β-strands in its long straight fibrils formed under acidic conditions comes from magic angle spinning NMR [37] and electron paramagnetic resonance experiments [38]. In addition, the latter report also demonstrates that the WL particles of β_2m do not adopt a parallel arrangement. Furthermore, a comparative IR study of the amide I band characteristics by Radford's group shows that the β-sheet architecture in amyloid fibrils formed *in vitro* at low, as well as at neutral pH, from recombinant β_2m is indistinguishable from their *ex vivo* counterparts, highlighting a common amyloid fold [52].

Beside the major fibril-specific IR spectral features discussed above, a further spectral attribute (at 1662 cm^{-1}) appears upon fibril formation at neutral pH (Fig. 4B), is well-defined in the final state of β_2m-F^{Phys} (Fig. 4D), and is also present in the spectrum of β_2m-F^{Acid} (Fig. 7B). A comparable characteristic can also be observed in the spectra of LS fibrils of the hamster prion protein, but not in the spectra of its curvy S-like fibrils [53,54]. This band component may reflect a characteristic arrangement of β-stands in LS fibrils of both proteins. Theoretical calculations indicate that both the number of strands in a β-sheet and local conformational disorder impact on the spectral features in the amide I region [40,41,55–57]. It thus appears possible that the band component at ~1662 cm^{-1} observed by us could be an indicator of these structural features. In line with this, the appearance of a spectral component in the 1660–1670 cm^{-1} region has been predicted at the high wavenumber side of the dominating low-frequency β-sheet band upon sheet deformation [41,57]. Despite these considerations, we regard the assignment of this spectral feature presently as uncertain, as its presence cannot be explained based on established structure–spectrum correlations for natively folded proteins. Apart from uncertainties in its assignment, it remains to be seen whether a pronounced spectral attribute in the 1660–1670 cm^{-1} region is highly characteristic for the IR spectra of LS amyloid fibrils in general.

All the structural changes observed by IR spectroscopy provide evidence for a major re-organization on the level of secondary structure upon conversion from the native to the final fibrillar structure of β_2m. In addition to that, independent support for a significant structural rearrangement upon the conversion of β_2m is provided by the spectral changes of the absorption band of the tyrosine side chain at ~1515 cm^{-1}, which is a sensitive local monitor of protein tertiary structure [30,32]. There are six tyrosine residues in β_2m, of which five form a cluster in the natively folded protein, while one residue is located apart from this cluster. The shift of the peak position of the tyrosine band by more than one wavenumber upon transition from the native to the fibril state (Fig. 4C) is highly significant, demonstrating that all tyrosine residues experience changes in their microenvironment as a consequence of the conversion process. This band shift provides clear-cut evidence against the existence of a native-like tyrosine cluster in amyloid fibrils of β_2m.

These data are in contrast to a recent solid state NMR study [58], which suggests that the final β_2m fold observed in mature fibrils appears to be similar to that in the native structure. The reasons for

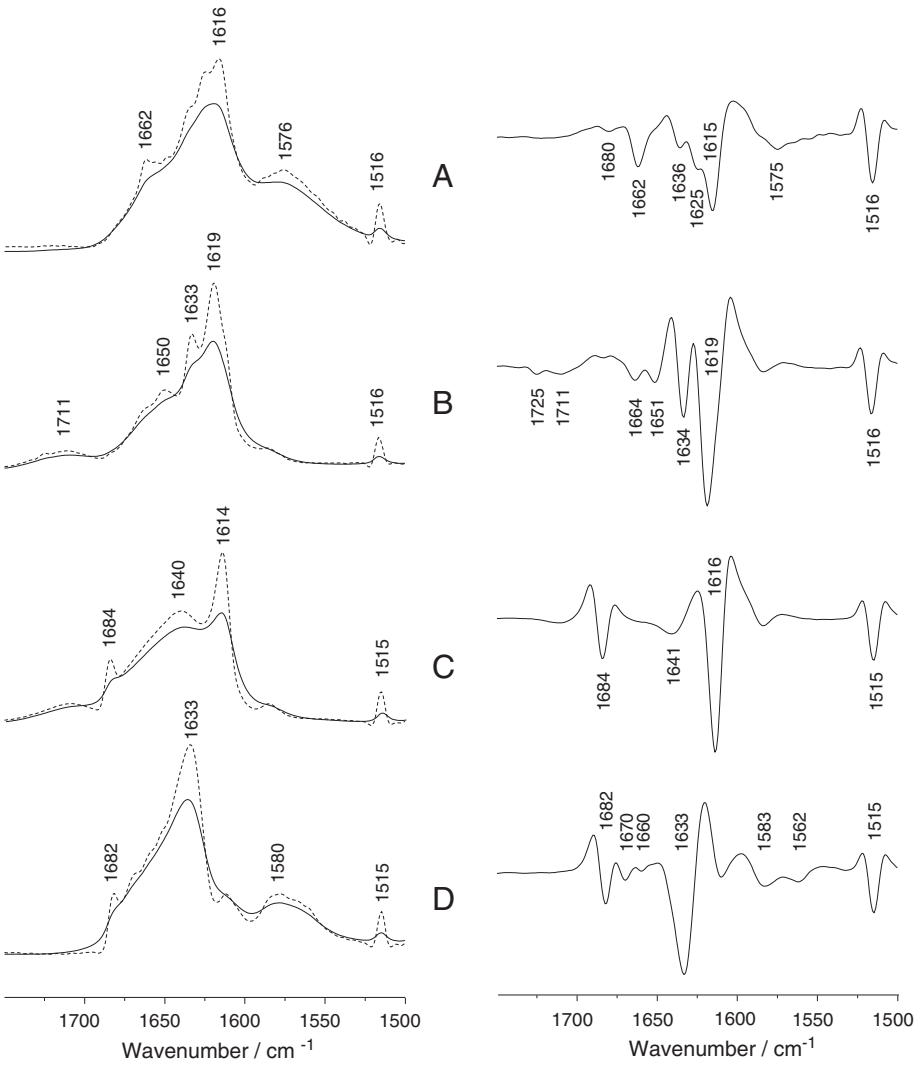

Fig. 7. Infrared spectra of various forms of β_2m. IR absorbance spectra (solid lines) and their spectra after band-narrowing by Fourier self-deconvolution (dashed lines), respectively (left side) and the corresponding second-derivative spectra (right side) of different forms of fully deuterated β_2m. (A) Stirring-induced long straight fibrils of β_2m in the presence of 1 M NaCl at neutral pH; (B) stirring-induced long straight fibrils of β_2m in the presence of 0.05 M NaCl at pH 2.1 (IR data taken from previous work by our group, see Ref. [28]); (C) worm-like assemblies of β_2m obtained in the presence of 0.2 M NaCl at pH 2.1 (IR data taken from previous work by our group, see Ref. [29]); (D) Natively folded β_2m at neutral pH.

the totally different conclusions derived from this report, on one side, and those obtained by magic angle spinning NMR [37], electron paramagnetic resonance experiments [38] and our IR spectroscopic study, on the other side, are not obvious. In contrast to the three latter studies, Pintacuda and co-workers [58] prepared their fibrils at neutral pH in the presence of 20% 2,2,2,-trifluoroethanol (TFE). Under these conditions, fibril formation of β_2m proceeds to intermediates(s), which are specific for moderate concentrations of TFE [59–61], although the morphology of these fibrils varies only slightly depending on the solvent conditions [59]. Thus, the question remains whether the secondary structure of fibrillar β_2m assemblies formed in the presence of 20% aqueous TFE at neutral pH is really indistinguishable from those obtained in the absence of TFE. In this context further previous studies deserve mention, which have identified and characterized native-like oligomeric species as intermediate aggregates of β_2m [62,63]. A highly non-native like parallel arrangements of β-strands in the amyloid fibrils of β_2m, that are present both at acidic and neutral pH conditions (29 and present work), cast doubts on the suitability of oligomeric motifs of β_2m with a native-like antiparallel β-sheet conformation as an atomic model for the building blocks of mature fibril form(s) of β_2m.

Another observation currently escaping molecular explanation is the coexistence of amorphous and thin filamentous structures at the end of the lag phase following the initiation of fibril formation (Fig. 5B). These filamentous structures could represent intermediates upon the conversion from the native-like to the non-native like parallel arrangement of the β-stands in the amyloid fibrils. Unfortunately, the IR techniques applied in this work provide only averaged structural information over all the molecules in the IR beam, which cannot be extrapolated to individual particles. The use of emerging techniques that provide structural information on the nanoscale range, such as tip-enhanced Raman spectroscopy [64,65] or near-field infrared microscopy [66], could provide novel and deeper insights into early conformational changes associated with fibril formation of β_2m.

In conclusion, we provide a highly efficient procedure for β_2m amyloid formation *in vitro* that appears simpler than others described before. As it involves the application of elevated temperatures and high ionic strength, it still cannot be considered physiological. However, it avoids the use of diverse auxiliary substances during fibril formation as well as the application of strongly acidic conditions [9–21,29,33] and permits the analysis of β_2m conversion from the native to the

fibrillar state using spectroscopic techniques as well as electron microscopy. Our procedure should therefore be suitable for further studies of β_2m amyloidogenesis.

Acknowledgments

We are grateful to Dr. Hans Huser for help with the β_2m preparations, to Dr. Ralph Golbik for the pseudo-wild-type barstar mutant C40A/C82A/P27A and to Janett Piesker for performing some of the EM preparations. This work was supported by the Deutsche Forschungsgemeinschaft (grants Fa 320/7-3, Na 226/12-2, UC8/1-2 and 2-1, and SFB 449 TP B6).

Appendix A. Supplementary data

Supplementary data to this article can be found online at http://dx.doi.org/10.1016/j.bpc.2013.05.001.

References

[1] P.J. Bjorkman, M.A. Saper, B. Samraoui, W.S. Bennett, J.L. Strominger, D.C. Wiley, Structure of the human class I histocompatibility antigen HLA-A2, Nature 329 (1987) 506–512.
[2] J.W. Becker, G.N. Reeke Jr., Three dimensional structure of β_2-microglobulin, Proceedings of the National Academy of Sciences of the United States of America 82 (1985) 4225–4229.
[3] F. Gejyo, T. Yamada, S. Odani, Y. Nakagawa, M. Arakawa, T. Kunitomo, H. Kataoka, M. Suzuki, Y. Hirasawa, T. Shirahama, A.S. Cohen, K. Schmid, A new form of amyloid protein associated with chronic hemodialysis was identified as β_2-microglobulin, Biochemical and Biophysical Research Communications 129 (1985) 701–706.
[4] P.D. Gorevic, T.T. Casey, W.J. Stone, C.R. Diraimondo, F.C. Prelli, B. Frangione, β_2-microglobulin is an amyloidogenic protein in man, Journal of Clinical Investigation 76 (1985) 2425–2429.
[5] N.H.H. Heegaard, β_2-Microglobulin: from physiology to amyloidosis, Amyloid 16 (2009) 151–173.
[6] T. Eichner, S.E. Radford, Understanding the complex mechanisms of β_2-microglobulin amyloid assembly, FEBS Journal 278 (2011) 3868–3883.
[7] S.E. Radford, W.S. Gosal, G.W. Platt, Towards an understanding of the structural molecular mechanism of β_2-microglobulin amyloid formation in vitro, Biochimica et Biophysica Acta 1753 (2005) 51–63.
[8] T. Eichner, A.P. Kalverds, G.S. Thompson, S.W. Homanns, S.E. Radford, Conformational conversion during amyloid formation at atomic resolution, Molecular Cell 41 (2011) 161–172.
[9] C.J. Morgan, M. Gelfand, C. Atreya, A.D. Miranker, Kidney dialysis-associated amyloidosis: a molecular role for copper in fiber formation, Journal of Molecular Biology 309 (2001) 339–345.
[10] M.F. Calabrese, C.M. Eakin, J.M. Wang, A.D. Miranker, A regulatable switch mediates self-association in an immunoglobulin fold, Nature Structural & Molecular Biology 15 (2008) 965–971.
[11] V.N. Mendoza, M.A. Baron-Rodriguez, C. Blanco, R.W. Vachet, Structural insights into the pre-amyloid tetramer of β_2-microglobulin from covalent labeling and mass spectrometry, Biochemistry 50 (2011) 6711–6722.
[12] A. Relini, C. Canale, S. DeStefano, R. Rolandi, S. Giorgetti, M. Stoppini, A. Rossi, F. Fogolari, A. Corazza, G. Esposito, A. Gliozzi, V. Belotti, Collagen plays an active role in the aggregation of β_2-microglobulin under physiopathological conditions of dialysis-related amyloidosis, Journal of Biological Chemistry 281 (2006) 16521–16529.
[13] S. Yamamoto, I. Yamaguchi, K. Hasegawa, S. Tsutsumi, Y. Goto, F. Gejyo, H. Naiki, Glycosaminoglycans enhance the trifluoroethanol-induced extension of β_2-microglobulin-related amyloid fibrils at a neutral pH, Journal of the American Society of Nephrology 15 (2004) 126–133.
[14] A.J. Borysik, I.J. Morten, S.E. Radford, E.W. Hewitt, Specific glycosaminoglycans promote unseeded amyloid formation from β_2-microglobulin under physiological conditions, Kidney International 72 (2007) 174–181.
[15] H. Pal-Gabor, L. Gombos, A. Misconai, E. Kovacs, E. Petrik, J. Kovacs, L. Graf, J. Fidy, H. Naiki, Y. Goto, K. Liliom, J. Kardos, Mechanism of lysophosphatidic acid-induced amyloid fibril formation of β_2-microglobulin *in vitro* under physiological conditions, Biochemistry 48 (2009) 5689–5699.
[16] T. Ookoshi, K. Hasegawa, Y. Okhashi, H. Kimura, N. Takahashi, R. Miyazaki, Y. Goto, H. Naiki, Lysophospholipids induce nucleation and extension of β_2-microglobulin-related amyloid fibrils at neutral pH, Nephrology Dialysis Transplantant 23 (2008) 3247–3255.
[17] K. Hasegawa, S. Tsutsumi-Yamsuhara, T. Ookoshi, Y. Ohhashi, H. Kimura, N. Takahashi, H. Yoshida, R. Miyazaki, Y. Goto, H. Naiki, Growth of β_2-microglobulin-related amyloid fibrils by non-esterified fatty acids at neutral pH, Biochemical Journal 416 (2008) 307–315.
[18] S.L. Myers, S. Jones, T.R. Jahn, I.J. Morten, G.A. Tennent, E.W. Hewitt, S.E. Radford, A systematic study of the effect of physiological factors on β_2-microglobulin amyloid formation at neutral pH, Biochemistry 45 (2006) 2311–2321.
[19] S. Yamamoto, K. Hasegawa, I. Yamaguchi, S. Tsutsumi, J. Kardos, Y. Goto, F. Gejyo, H. Naiki, Low concentrations of sodium dodecyl sulfate induce the extension of β_2-microglobulin-related amyloid fibrils at neutral pH, Biochemistry 43 (2004) 11075–11082.
[20] Y. Ohhashi, M. Kihara, H. Naiki, Y. Goto, Ultrasonication-induced amyloid fibril formation of β_2-microglobulin, Journal of Biological Chemistry 280 (2005) 32843–32848.
[21] M. Kihara, E. Catani, K. Sakai, K. Hasegawa, H. Naiki, Y. Goto, Seeding-dependent maturation of β_2-microglobulin amyloid fibrils at neutral pH, Journal of Biological Chemistry 280 (2005) 12012–12018.
[22] K. Sasahara, H. Yagi, H. Naiki, Y. Goto, Heat-induced conversion of β_2-microglobulin and hen egg-white lysozyme into amyloid fibrils, Journal of Molecular Biology 372 (2007) 981–991.
[23] K. Sasahara, H. Yagi, M. Sakai, H. Naiki, Y. Goto, Amyloid nucleation triggered by agitation of β_2-microglobulin under acidic and neutral pH conditions, Biochemistry 47 (2008) 2650–2660.
[24] M. Hülsmeyer, R.C. Hillig, A. Volz, M. Rühl, W. Schröder, W. Saenger, A. Ziegler, B. Uchanska-Ziegler, HLA-B27 subtypes differentially associated with disease exhibit structural alterations, Journal of Biological Chemistry 279 (2002) 47844–47852.
[25] K. Sasahara, H. Yagi, H. Naiki, Y. Goto, Heat-triggered conversion of protofibrils into mature amyloid fibrils of β_2-microglobulin, Biochemistry 46 (2007) 3286–3293.
[26] H. Fabian, W. Mäntele, in: J.M. Chalmers, P.R. Griffiths (Eds.), Handbook of Vibrational Spectroscopy, Infrared Spectroscopy of Proteins, Wiley, Chichester, 2002, p. 3399.
[27] J. Zhang, Y.B. Yan, Probing conformational changes of proteins by quantitative second-derivative infrared spectroscopy, Analytical Biochemistry 340 (2005) 89–98.
[28] K. Gast, A. Nöppert, M. Müller-Frohne, D. Zirwer, G. Damaschun, Stopped-flow dynamic light scattering as a method to monitor compaction during protein folding, European Biophysical Journal 25 (1997) 211–219.
[29] H. Fabian, K. Gast, M. Laue, R. Misselwitz, B. Uchanska-Ziegler, A. Ziegler, D. Naumann, Early stages of misfolding and association of β_2-microglobulin: insights from infrared spectroscopy and dynamic light scattering, Biochemistry 47 (2008) 6895–6906.
[30] H. Fabian, H. Huser, D. Narzi, R. Misselwitz, B. Loll, A. Ziegler, R.A. Böckmann, B. Uchanska-Ziegler, D. Naumann, HLA-B27 subtypes differentially associated with disease exhibit conformational differences in solution, Journal of Molecular Biology 376 (2008) 798–810.
[31] J. Kardos, D. Okuno, T. Kawai, Y. Hagihara, N. Yumoto, T. Kitagawa, P. Zavodszky, H. Naiki, Y. Goto, Structural studies reveal that the diverse morphology of β_2-microglobulin aggregates is a reflection of different molecular architectures, Biochimica et Biophysica Acta 1753 (2005) 108–120.
[32] H. Fabian, C. Schultz, J. Backmann, U. Hahn, W. Saenger, H.H. Mantsch, D. Naumann, Impact of point mutations on the structure and thermal stability of ribonuclease T1 in aqueous solution probed by Fourier transform infrared spectroscopy, Biochemistry 33 (1994) 10725–10730.
[33] H.E. White, J.L. Hodgkinson, T.R. Jahn, S. Cohen-Krausz, W.S. Gosal, S. Müller, E.V. Orlova, S.E. Radford, H.R. Saibel, Globular tetramers of ß$_2$-microglobulin assemble into elaborate amyloid fibrils, Journal of Molecular Biology 389 (2009) 48–57.
[34] M.F. Mossuto, A. Dhulesia, G. Devlin, E. Frare, J.R. Kumita, P. Polverino de Laureto, M. Dumoulin, A. Fontana, C.M. Dobson, X. Salvatella, The none-core regions of human lysozyme amyloid fibrils influence cytotoxicity, Journal of Molecular Biology 402 (2010) 783–796.
[35] B. Nölting, R. Golbik, A.R. Fersht, Submillisecond events in protein folding, Proceedings of the National Academy of Sciences of the United States of America 92 (1995) 10668–10672.
[36] M.S. Celej, R. Sarroukh, E. Goormaghtigh, G.D. Fidelo, J.-M. Ruysschaert, V. Raussens, Toxic prefibrillar α-synuclein amyloid oligomers adopt a distinctive antiparallel β-sheet structure, Biochemical Journal 443 (2012) 719–726.
[37] G.T. Debelouchina, G.W. Platt, M.J. Bayro, S.E. Radford, R.G. Griffin, Intermolecular alignment in β_2-microglobulin amyloid fibrils, Journal of the American Chemical Society 132 (2010) 17077–17079.
[38] C.L. Ladner, M. Chen, D.P. Smith, G.W. Platt, S.E. Radford, R. Langen, Stacked sets of parallel, in-register β-strands of β_2-microglobulin in amyloid fibrils revealed by site-directed spin labelling and chemical labelling, Journal of Biological Chemistry 285 (2010) 17137–17147.
[39] G. Zandomeneghi, M.R.H. Krebs, M.C. Mc Cammon, M. Fändrich, FTIR reveals structural differences between native β-sheet proteins and amyloid fibrils, Protein Science 13 (2004) 3314–3321.
[40] J. Kubelka, T. Keiderling, The anomalous infrared amide I intensity distribution in C-13 isotopically labelled peptide b-sheets comes from extended, multiple-stranded structures. An ab initio study, Journal of the American Chemical Society 123 (2001) 6142–6150.
[41] N. Demirdöven, C.M. Cheatum, H.S. Chung, M. Khalil, A. Tokmakoff, Two-dimensional infrared spectroscopy of antiparallel β-sheet secondary structure, Journal of the American Chemical Society 126 (2004) 7981–7990.
[42] E.-L. Karjalainen, H.K. Ravi, A. Barth, Simulation of the amide I absorption of stacked β-sheets, The Journal of Physical Chemistry. B 115 (2011) 749–757.
[43] M. Bouchard, J. Zurdo, E.I. Nettleton, C.M. Dobson, C.V. Robinson, Formation of insulin amyloid fibrils followed by FTIR simultaneously with CD and electron microscopy, Protein Science 9 (2000) 1960–1967.
[44] I. de la Arada, C. Seiler, W. Mäntele, Amyloid fibril formation from human and bovine serum albumin followed by quasi-simultaneous Fourier-transform infrared (FT-IR) and static light scattering (SLS), European Biophysics Journal 41 (2012) 931–938.
[45] J. Zurdo, J.I. Guijarro, J.L. Jiminez, H.R. Saibil, C.M. Dobson, Dependence on solution conditions of aggregation and amyloid formation by an SH3 domain, Journal of Molecular Biology 311 (2001) 325–340.
[46] J. Zurdo, J.I. Guijarro, C.M. Dobson, Preparation and characterization of purified amyloid fibrils, Journal of the American Chemical Society 123 (2001) 8141–8142.

[47] E. Frare, M.F. Mossuto, P. Polverino de Laureto, M. Dumoulin, C.M. Dobson, A. Fontana, Identification of the core structure of lysozyme amyloid fibrils by proteolysis, Journal of Molecular Biology 361 (2006) 551–561.
[48] E. Cerf, R. Sarroukh, S. Tamamizu-Kato, L. Breydo, S. Derclayes, Y.F. Dufrenes, V. Narayanaswan, E. Goormaghtigh, J.-M. Ruysschaert, V. Raussens, Antiparallel β-sheet: a signature of the oligomeric amyloid β-peptide, Biochemical Journal 421 (2009) 415–423.
[49] M. Fändrich, Oligomeric intermediates in amyloid formation: structure determination and mechanisms of toxicity, Journal of Molecular Biology 421 (2012) 427–440.
[50] K. Janek, J. Behlke, J. Zipper, H. Fabian, Y. Georgalis, M. Beyermann, M. Bienert, E. Krause, Water-soluble β-sheet models which self-assemble into fibrillar structures, Biochemistry 38 (1999) 8246–8252.
[51] K. Yamaguchi, S. Takahashi, T. Kawai, H. Naiki, Y. Goto, Seeding-dependent propagation and maturation of amyloid fibril formation, Journal of Molecular Biology 352 (2005) 952–960.
[52] T.R. Jahn, G.A. Tennet, S.E. Radford, A common β-sheet architecture underlies in vitro and in vivo β_2-microglobulin amyloid fibrils, Journal of Biological Chemistry 283 (2008) 17279–17286.
[53] O.V. Bocharova, L. Breydo, A.S. Parfenov, V.V. Salnikov, I.V. Baskakov, In vitro conversion of full-length mammalian prion protein produces amyloid form with physical properties of PrP^{Sc}, Journal of Molecular Biology 346 (2005) 645–659.
[54] N. Makara, I.V. Baskakov, The same primary structure of the prion protein yields two distinct self-propagating states, Journal of Biological Chemistry 283 (2008) 15988–15996.
[55] J. Kubelka, T.A. Keiderling, Differentiation of β-sheet forming structures: ab initio-based simulations of IR absorption and vibrational CD for model peptide and protein β-sheets, Journal of the American Chemical Society 123 (2001) (2001) 12048–12058.
[56] J.W. Brauner, C.R. Flach, R. Mendelsohn, A quantitative reconstitution of the amide I contour in the IR spectra of globular proteins: from structure to spectrum, Journal of the American Chemical Society 127 (2005) 100–109.
[57] R. Schweitzer-Stenner, Simulated IR, isotropic and anisotropic Raman, and vibrational circular dichroism amide I band profiles of stacked β-sheets, The Journal of Physical Chemistry. B 116 (2012) 4141–4153.
[58] E. Barbet-Massin, S. Ricagno, J.R. Lewandowski, S. Giorgetti, V. Bellotti, M. Bolognesi, L. Emsley, G. Pintacuda, Fibrillar vs crystalline full-length β_2-microglobulin studied by high-resolution solid-state NMR spectroscopy, Journal of the American Chemical Society 132 (2010) 5556–5557.
[59] E. Renella, A. Corazza, S. Giorgetti, F. Fogolari, P. Viglino, R. Porcari, L. Verga, M. Stoppini, V. Belotti, G. Esposito, Folding and fibrillogenesis: clues from β_2-microglobulin, Journal of Molecular Biology 401 (2010) 286–297.
[60] K. Yamamoto, H. Yagi, Y.-H. Lee, Y. Hagihara, H. Naiki, Y. Goto, The amyloid fibrils of the constant domain of immunoglobulin light chain, FEBS Letters 584 (2010) 3348–3353.
[61] C. Santambrogio, S. Ricagno, F. Sobott, M. Colombo, M. Bolognesi, R. Grandori, Characterization of β_2m-microglobulin conformational intermediates associated to different fibrillation conditions, Journal of Mass Spectrometry 46 (2011) 734–741.
[62] C. Liu, M.R. Sawaya, D. Eisenberg, β_2-Microglobulin forms three-dimensional domain-swapped amyloid fibrils with disulfide linkages, Nature Structural & Molecular Biology 18 (2011) 49–55.
[63] C.M. Eakin, A.J. Berman, A.D. Miranker, A native to amyloidogenic transition regulated by a backbone trigger, Nature Structural Biology 13 (2006) 202–208.
[64] P. Hermann, H. Fabian, D. Naumann, A. Hermelink, Comparative study of far-field and near-field Raman spectra from silicon-based samples and biological nanostructures, Journal of Physical Chemistry 115 (2011) 24512–24520.
[65] T. Deckert-Gauding, E. Kämmer, V. Deckert, Tracking of nanoscale structural variations on a single amyloid fibril with tip-enhanced Raman scattering, Journal of Biophotonics 5 (2012) 215–219.
[66] M. Paulite, Z. Fakhraai, I.T.S. Li, N. Gunari, A.E. Tanur, G.C. Walker, Imaging secondary structure of individual amyloid fibrils of a β_2-microglobulin fragment using near-field infrared spectroscopy, Journal of the American Chemical Society 133 (2011) 7376–7383.